

A Nucleophilic Chromium(V) Dioxo Radical Anion

Aaron L. Odom, Daniel J. Mindiola, and Christopher C. Cummins*

Department of Chemistry, Massachusetts Institute of Technology, Cambridge, Massachusetts 02139

Received December 8, 1998

Treatment of $\text{Cr}(\text{NRAr})_3$ ($\text{R} = \text{C}(\text{CD}_3)_2\text{CH}_3$ or *tert*-butyl, $\text{Ar} = 2,5\text{-C}_6\text{H}_3\text{FMe}$) with oxygen gives the purple chromium(VI) complex $\text{O}_2\text{Cr}(\text{NRAr})_2$ in 83% purified yield. Upon one-electron reduction with cobaltocene, the d^1 dioxo cobaltocenium salt $[\text{CoCp}_2][\text{O}_2\text{Cr}(\text{NRAr})_2]$ was isolated in 89% yield. The dioxo anion displays solid-state magnetic behavior consistent with a Curie–Weiss paramagnet with one unpaired electron. The chromium(V) dioxo $[\text{CoCp}_2][\text{O}_2\text{Cr}(\text{NRAr})_2]$ acts as a nucleophile toward ClSiPh_3 , $\text{ClC}(\text{O})\text{Ph}$, and MeOTf to afford the monooxo complexes $\text{OCr}(\text{OSiPh}_3)(\text{NRAr})_2$ (86% yield), $\text{OCr}[\text{OC}(\text{O})\text{Ph}](\text{NRAr})_2$ (34% yield), and $\text{OCr}(\text{OMe})(\text{NRAr})_2$ (76% yield), respectively. Two of these rare examples of monooxo chromium(V) derivatives, $\text{OCr}(\text{OSiPh}_3)(\text{NRAr})_2$ and $\text{OCr}[\text{OC}(\text{O})\text{Ph}](\text{NRAr})_2$, were structurally characterized and display $\text{Cr}-\text{O}_{\text{oxo}}$ distances of 1.611(6) and 1.588(3) Å, respectively. The benzoate complex features an η^1 -carboxylate ligand. All of the monooxo complexes show three peaks in their ^2H NMR spectra consistent with isomers arising from restricted rotation about the $\text{Cr}-\text{N}$ bonds. Two of the complexes, $\text{O}_2\text{Cr}(\text{NRAr})_2$ and $\text{OCr}(\text{OSiPh}_3)(\text{NRAr})_2$, were examined by cyclic voltammetry.

1. Introduction

The chemistry of metal dioxo compounds has developed steadily over several decades. The impetus for recent activity concerning this class of complexes has come from the bioinorganic and coordination chemistry of these compounds. The existence of oxo motifs in the enzymes of some organisms has elicited a rapid elaboration of biologically relevant chemistry of molybdenum and tungsten oxo species.^{1,2} In addition, methodologies for the synthesis of *cis*-dioxo complexes with one or two unpaired electrons^{3–8} have developed with possible implications for the rapidly expanding field of organic substrate oxidation.⁹

Synthetic approaches to the synthesis of *cis*-dioxo complexes have utilized facial-tridentate ligands to favor the desired *cis* geometry of the dioxo unit. For example, hydrotris(1-pyrazolyl)-

borate and its derivatives $[\text{HB}(\text{pz})_3^-]$ have been employed for this purpose in the synthesis of $[\text{HB}(\text{pz})_3]\text{ReO}_2\text{Cl}^4$ and $[\text{HB}(\text{pz})_3]\text{MoO}_2(\text{SPh})^-$.³ *cis*-Dioxo complexes that do not incorporate such tridentate ligands also have been reported^{6–8} and have been the subject of theoretical studies.¹⁰ Examples include the surprising d^2 compounds $\text{OsO}_2(\text{O}_2\text{CMe})_3^-$ and $\text{RuO}_2\text{Cl}_2(\text{O}_2\text{CMe})^-$.^{7,8}

A few rare examples of pseudotetrahedral dioxo compounds with d^n ($n > 0$) also have been prepared. The only previously published members of this category were provided by Wilkinson and co-workers in the form of $\text{O}_2\text{Re}(\text{aryl})_2$ and $\text{O}_2\text{Os}(\text{aryl})_2$ ($\text{aryl} = 2,4,6\text{-trimethylphenyl}$ or $2,6\text{-dimethylphenyl}$).⁵

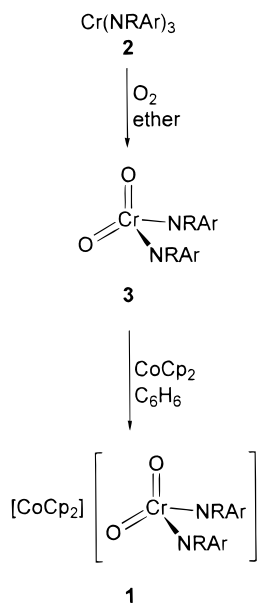
Unprecedented in the chemistry of 4-coordinate dioxo metal complexes are examples from the first row of the transition series manifesting the d^1 electronic configuration. In this paper, we present the detailed synthesis of the d^1 dioxo $[\text{CoCp}_2][\text{O}_2\text{-Cr}(\text{NRAr})_2]$ (**1**) (where $\text{R} = \text{C}(\text{CD}_3)_2\text{CH}_3$ or *tert*-butyl, $\text{Ar} = 2,5\text{-C}_6\text{H}_3\text{FMe}$). Also, we include in this report the reactivity of this unique complex with various substrates, especially electrophiles, which can give rare examples of chromium(V) monooxo complexes in a pseudotetrahedral environment.

2. Results and Discussion

2.1. Synthesis of a Chromium(VI) Dioxo Complex. The reaction of excess dry oxygen with an ethereal solution of $\text{Cr}(\text{NRAr})_3$ (**2**), synthesized from 3 equiv of $(\text{Et}_2\text{O})\text{LiNRAr}$ and CrCl_3 in ether, caused a rapid color change from the green-brown of the starting material to dark purple. Isolation of the

- (1) Lorber, C.; Donahue, J. P.; Goddard, C. A.; Nordlander, E.; Holm, R. *J. Am. Chem. Soc.* **1998**, *120*, 8102–8112.
- (2) (a) Barnard, K. R.; Gable, R. W.; Wedd, A. G. *J. Biol. Inorg. Chem.* **1997**, *2*, 623–633. (b) Johnson, M. K.; Rees, D. C.; Adams, M. W. *Chem. Rev.* **1996**, *96*, 2817–2839. (c) Kletzin, A.; Adams, M. W. *FEMS Microbiol. Rev.* **1996**, *18*, 5.
- (3) Xiao, Z.; Gable, R. W.; Wedd, A. G.; Young, C. G. *J. Am. Chem. Soc.* **1996**, *118*, 2912–2921 and references therein.
- (4) DuMez, D. D.; Mayer, J. M. *Inorg. Chem.* **1998**, *37*, 445–453.
- (5) (a) Stavropoulos, P.; Edwards, P. G.; Behling, T.; Wilkinson, G.; Motevalli, M.; Hursthouse, M. B. *J. Chem. Soc., Dalton Trans.* **1987**, 169–175. (b) Longley, C. J.; Savage, P. D.; Wilkinson, G.; Hussain, B.; Hursthouse, M. B. *Polyhedron* **1988**, *7*, 1079–1088.
- (6) (a) Blackburn, R. L.; Jones, L. M.; Ram, M. S.; Sabat, M.; Hupp, J. T. *Inorg. Chem.* **1990**, *29*, 1791. (b) Herrmann, W. A.; Eder, S. J.; Scherer, W. *Angew. Chem., Int. Ed. Engl.* **1992**, *31*, 1345. (c) Herrmann, W. A.; Eder, S. J.; Scherer, W. *Chem. Ber.* **1993**, *126*, 39. (d) Conn, J. F.; Kim, J. J.; Suddath, F. L.; Blattmann, P.; Rich, A. *J. Am. Chem. Soc.* **1974**, *96*, 7152. (e) Johnson, J. W.; Brody, J. F.; Ansell, G. B.; Zentz, S. *Inorg. Chem.* **1984**, *23*, 2415. (f) Lau, T. C.; Kochi, J. K. *J. Chem. Soc., Chem. Commun.* **1987**, 798. (g) Perrier, S.; Lau, T. C.; Kochi, J. K. *Inorg. Chem.* **1990**, *29*, 4190.
- (7) Behling, T.; Capparelli, M. V.; Skapski, A. C.; Wilkinson, G. *Polyhedron* **1982**, *1*, 840.
- (8) Griffith, W. P.; Jolliffe, J. M.; Ley, S. V.; Williams, D. J. *J. Chem. Soc., Chem. Commun.* **1990**, 1219.

- (9) (a) Cainelli, G.; *Chromium Oxidation in Organic Chemistry*; Springer-Verlag: Berlin, 1984. (b) Sheldon, R. A.; Kochi, J. K. *Metal-Catalyzed Oxidation of Organic Compounds*; Academic Press: New York, 1981. (c) Mijs, W. J.; de Jonge, C. R. H. I. *Organic Syntheses by Oxidation with Metal Compounds*; Plenum Press: New York, 1986. (d) Patterson, R. E.; Gordon-Wylie, S. W.; Woome, C. G.; Norman, R. E.; Weintraub, S. T.; Horwitz, C. P.; Collins, T. J. *Inorg. Chem.* **1998**, *37*, 4748–4750 and references therein.
- (10) Demanchy, I.; Jean, Y. *Inorg. Chem.* **1996**, *35*, 5027–5031.

Scheme 1. Synthesis of a 4-Coordinate 3d¹ Dioxo Complex

purple product by recrystallization from pentane or ether removed the amine byproduct, giving $\text{O}_2\text{Cr}(\text{NRAr})_2$ (**3**) in 83% yield (Scheme 1).

Two other studies involving the reaction of oxygen with chromium(III) amido complexes have appeared in the literature. Bradley and co-workers studied the reaction of oxygen with $\text{Cr}(\text{N-}i\text{-Pr})_2$ utilizing EPR spectroscopy.¹¹ The reaction reportedly proceeds with the loss of an amido group as the radical $\text{ON-}i\text{-Pr}_2$ to give the chromium(VI) product $\text{O}_2\text{Cr}(\text{N-}i\text{-Pr})_2$.¹² More recently, Gambarotta and co-workers reported the reaction of $\text{Cr}(\text{NAdAr}')_3$ (Ad = 1-adamantyl, Ar' = 3,5-dimethylphenyl) with oxygen.¹³ A product analogous to **3**, $\text{O}_2\text{Cr}(\text{NAdAr}')_2$, was isolated in 80% yield. In addition, the reduced product $[(\mu\text{-O})\text{-Cr}(\text{NAdAr}')_2]_2$ was isolated from reactions of $\text{O}_2\text{Cr}(\text{NAdAr}')_2$ with $\text{P}(\text{C}_6\text{H}_{11})_3$.

Pure samples of $\text{O}_2\text{Cr}(\text{NRAr})_2$ (**3**) display two isomers as interrogated by solution ¹H NMR. The two isomers are explicable in terms of hindered rotation about the Cr–N_{amido} bonds. Figure 1 portrays graphically the two isomers in terms of C₂/C_s symmetric variance. Similar electronic effects resulting in restricted rotation around Cr(VI)–N_{amido} bonds have been reported previously.¹⁴ While no observable isomerism was mentioned for the complexes $\text{O}_2\text{Cr}(\text{NAdAr}')_2$ and $\text{O}_2\text{Cr}[\text{N}(\text{C}_6\text{H}_{11})_2]_2$,¹³ the ¹H NMR resonances for the chromium(VI) complexes were cited as being broad, which is possibly indicative of slow rotation around Cr–N_{amido} bonds in these derivatives.

Crystals appropriate for X-ray diffraction experiments were obtained by cooling an ethereal solution of $\text{O}_2\text{Cr}(\text{NRAr})_2$ (**3**). The sample selected contained the C₂ symmetric isomer (Figure 1). An X-ray structural determination (Figure 2) on **3** indicates short metal–oxygen bonds of 1.592(2) Å. Also, the complex has an average Cr–N_{amido} distance of 1.837(3) Å. The characteristics of the Cr(VI)–N_{amido} bonds in **3** are reminiscent of chromium(VI) nitrido complexes, where amido substituents

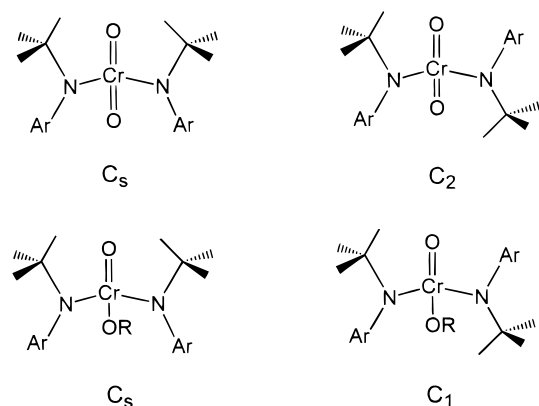


Figure 1. The NMR spectroscopy of the chromium bis(amido) complexes is indicative of slow Cr–N_{amido} rotation on the NMR time scale. The ¹H NMR spectrum of $\text{O}_2\text{Cr}(\text{NRAr})_2$ (**3**) is explicable in terms of two isomers of approximate C_s and C₂ symmetry. The ²H NMR spectra of $\text{OCr}(\text{OR})(\text{NRAr})_2$ (**4b**) (for example in R = SiPh₃) display three resonances, indicative of two isomers of approximate C_s and C₁ symmetry.

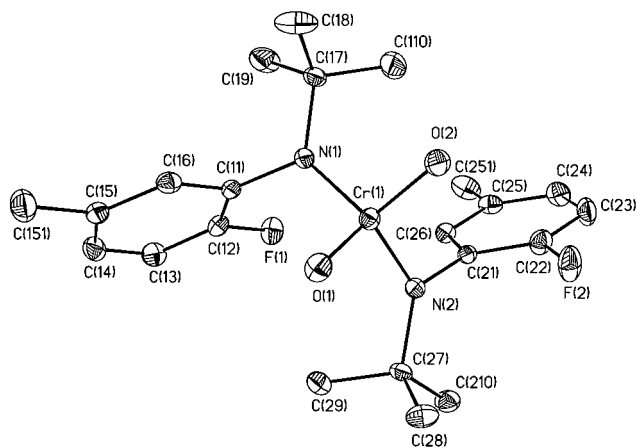


Figure 2. ORTEP diagram from the X-ray crystal structure data for $\text{O}_2\text{Cr}(\text{NRAr})_2$ (**3**). The ellipsoids are at the 25% probability level. Selected distances (Å): Cr1–O1 1.591(2), Cr1–O2 1.592(2), Cr1–N1 1.844(2), Cr1–N2 1.829(3). Selected angles (deg): O1–Cr1–O2 113.35(12), O1–Cr1–N2 107.58(11), O2–Cr1–N2 108.50(11), O1–Cr1–N1 108.72(11), O2–Cr1–N1 107.42(11), N2–Cr1–N1 111.32(11).

often show significant Cr–N_{amido} multiple bond character and correspondingly shortened Cr–N_{amido} bond distances.¹⁴

The strongly π -donating amido substituents result in a Cr(VI) metal center that is quite electron-rich. The electron-rich nature of **3** is manifested in its lack of reactivity with a number of oxidizable substrates including tetrahydrothiophene and norbornylene. Cyclic voltammetry on **3** in THF suggests that the complex is difficult to reduce, with an $E_{1/2} = -1.04$ V relative to $\text{Cp}_2\text{Fe}^{+/0}$. The first reduction potential for **2** is similar to those reported for various alkylated pyrazolyl borate complexes of molybdenum, $[\text{HB}(\text{pz})_3]\text{MoO}_2(\text{SPh})^{0/-}$, which ranged from -1.11 to -0.98 V.³

2.2. Synthesis of a Chromium(V) Dioxo Complex. As displayed in Scheme 1, reaction of cobaltocene with $\text{O}_2\text{Cr}(\text{NRAr})_2$ (**3**) in benzene causes the rapid precipitation of a light-brown powder. On workup, the powder gave spectroscopically (²H NMR) pure $[\text{CoCp}_2][\text{O}_2\text{Cr}(\text{NRAr})_2]$ (**1**) in 89% yield. While the complex has not been structurally characterized, SQUID magnetometry on the complex is consistent with monomeric chromium centers in the solid state.

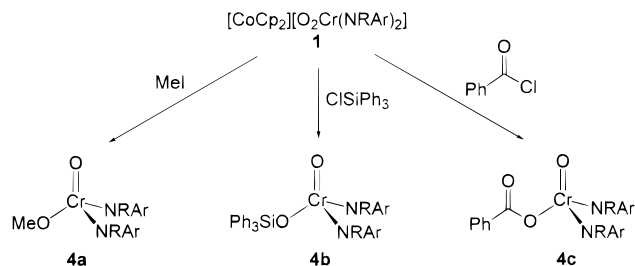
(11) Chien, J. C. W.; Kruse, W.; Bradley, D. C.; Newing, C. W. *Chem. Commun.* **1970**, 1177.

(12) Chisholm, M. H. Personal communication.

(13) Rупpa, K. B. P.; Feghali, K.; Kovaaacs, I.; Aparna, K.; Gambarotta, S.; Yap, G. P. A.; Bensimon, C. *J. Chem. Soc., Dalton Trans.* **1998**, 1595–1605.

(14) Odom, A. L.; Cummins, C. C. *Polyhedron* **1998**, *17*, 675–688.

Scheme 2. The Radical $[\text{CoCp}_2][\text{O}_2\text{Cr}(\text{NRAr})_2]$ (**1**) Reacts with Strong Electrophiles To Give Unusual Monooxo Chromium(V) 4-Coordinate Complexes



Syntheses of d^1 dioxo complexes by 1e reduction of d^0 complexes, in contrast with the synthesis of $[\text{CoCp}_2][\text{O}_2\text{Cr}(\text{NRAr})_2]$ (**1**), often are not successful due to fast valence and/or ligand disproportionation.³ The surprising thermal stability of **1** is attributable to the large number of π -donor ligands and the steric demands of the anilide ligands. The steric bulk of the amido substituents slows ligand and valence disproportionation by inhibiting bimolecular reactions. The low symmetry of **1** allows mixing of all π -donating orbitals. Therefore, the orbital containing the unpaired electron is diffuse, with π -antibonding character with respect to all four ligands. The result is a complex that is readily synthesized and isolated.

The d^1 dioxo complexes of group 6 stand in marked contrast to the Re d^1 dioxo reported by Mayer and co-workers.⁴ $[\text{HB}(\text{pz})_3]\text{ReO}_2\text{Cl}$ was found to have an oxidation potential 0.93 V cathodic of the ferrocene couple in CH_3CN . The enormous difference in $d^{0/1}$ cyclic voltammogram potentials between **3** and $[\text{HB}(\text{pz})_3]\text{ReO}_2\text{Cl}^+$ is mirrored in the differing reactivity of the complexes. While **3** shows no reactivity toward tetrahydrothiophene, $[\text{HB}(\text{pz})_3]\text{ReO}_2\text{Cl}^+$ has highly oxidizing oxo ligands. For example, $[\text{HB}(\text{pz})_3]\text{ReO}_2\text{Cl}^+$ readily oxidizes Me_2S to Me_2SO .⁴ Mayer and co-workers concluded that the highly *electrophilic* nature of $[\text{HB}(\text{pz})_3]\text{ReO}_2\text{Cl}^+$ was due in large part to its cationic charge. With this in mind, an elegant contrast to the Mayer work is revealed in the *nucleophilic* reaction chemistry of the anionic $[\text{CoCp}_2][\text{O}_2\text{Cr}(\text{NRAr})_2]$ (**1**) described below, and the reaction chemistry of **1** affords a unique set of Cr(V) monooxo complexes.

2.3. Reactivity of a Cr(V) Dioxo Complex. The conversion of oxo ligands to monoanionic substituents is a synthetic strategy that is increasingly being employed.^{1,3} For the most part, however, this strategy has only proved practicable in the synthesis of trialkylsilyloxy ligands. The use of $[\text{CoCp}_2][\text{O}_2\text{Cr}(\text{NRAr})_2]$ (**1**) as a nucleophile with methyl triflate, triphenylsilyl chloride, or benzoyl chloride led to the synthesis of monooxo complexes with heteroleptic basal ligand sets. The products are the unusual 4-coordinate monooxo complexes shown in Scheme 2. The radical **1** is strongly reducing, and the syntheses must employ electrophiles which are not prone to reduction.

The reaction of **1** with methyl triflate gave the dark blue, lipophilic complex $\text{OCr}(\text{OMe})(\text{NRAr})_2$ (**4a**) in 76% yield. The SQUID magnetometry data for **4a** revealed a susceptibility of $1.709(3) \mu_B$, very close to the spin-only value for one unpaired electron.

The reaction of ClSiPh_3 with the anion **1** produces the crystalline dark blue complex $\text{OCr}(\text{OSiPh}_3)(\text{NRAr})_2$ (**4b**) in 86% yield. The crystal structure of **4b** shows a $\text{Cr}-\text{O}_{\text{oxo}}$ distance of $1.611(6) \text{ \AA}$ (Figure 3). The $\text{Cr}-\text{O}_{\text{oxo}}$ distance in $\text{O}_2\text{Cr}(\text{NRAr})_2$ (**3**) of $1.592(2) \text{ \AA}$ is shorter than in **4b**, consistent with the higher formal oxidation state of the former.

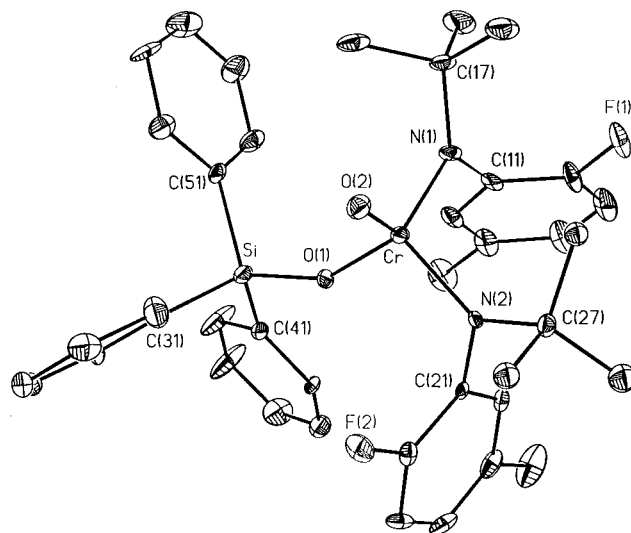


Figure 3. ORTEP diagram from the X-ray crystal structure data of $\text{OCr}(\text{OSiPh}_3)(\text{NRAr})_2$ (**4b**). There is a rotational disorder involving the *tert*-butyl group adjacent to N(2), and only one set of positions are shown. The ellipsoids are at the 25% probability level. Selected bond distances (\AA): $\text{Cr}-\text{O}_2$ 1.611(6), $\text{Cr}-\text{O}_1$ 1.792(6), $\text{Cr}-\text{N}_1$ 1.842(7), $\text{Cr}-\text{N}_2$ 1.847(7), $\text{Si}-\text{O}_1$ 1.637(6). Selected bond angles (deg): $\text{O}_2-\text{Cr}-\text{O}_1$ 110.9(3), $\text{O}_2-\text{Cr}-\text{N}_1$ 114.5(3), $\text{O}_1-\text{Cr}-\text{N}_1$ 109.1(3), $\text{O}_2-\text{Cr}-\text{N}_2$ 110.1(3), $\text{O}_1-\text{Cr}-\text{N}_2$ 103.3(3), $\text{N}_1-\text{Cr}-\text{N}_2$ 108.3(3), $\text{Si}-\text{O}_1-\text{Cr}$ 150.9(4), $\text{C}_{11}-\text{N}_1-\text{Cr}$ 113.6(5), $\text{C}_{17}-\text{N}_1-\text{C}_{17}$ 119.4(7), $\text{C}_{21}-\text{N}_2-\text{C}_{27}$ 115.7(6), $\text{C}_{21}-\text{N}_2-\text{Cr}$ 118.2(5), $\text{C}_{27}-\text{N}_2-\text{Cr}$ 115.7(6), $\text{C}_{21}-\text{N}_2-\text{Cr}$ 118.2(5).

Deuterium NMR spectra of the monooxo complexes, i.e., $\text{OCr}(\text{OSiPh}_3)(\text{NRAr})_2$ (**4b**), show three peaks (see Figure 1). These peaks are attributed to two different isomeric structures for the complexes as consequence of slow $\text{Cr}-\text{N}_{\text{amido}}$ rotation. Similar to dioxo **3**, complex **4b** elicits two isomers in solution approximating C_2 and C_s symmetries. These two isomers give rise to three different environments for the *tert*-butyl groups as observed in the ^2H NMR spectrum. This type of hindered rotation due to strong $\text{Cr}-\text{N}_{\text{amido}}$ π -bonding has been observed in other high oxidation state chromium amido complexes such as $\text{NCr}[\text{OC}(\text{CF}_3)_2\text{CH}_3](\text{N}-i\text{-Pr})_2$, where the barrier to amido rotation was found to be $\sim 16 \text{ kcal/mol}$.¹⁴

A third isomer of **4b** having both *tert*-butyl groups anti with respect to the oxo oxygen is also possible. However, no bis-(anilido)metal oxo or nitrido complexes with that arrangement of substituents have been characterized structurally. It is likely that this more sterically crowded isomer exists as a minor component of the solutions. Consequently, the isomer's concentration may be sufficiently small to prevent detection by NMR. Alternatively, the resonances may overlap with the broad peaks of the other isomers.

The monooxo complex $\text{OCr}(\text{OSiPh}_3)(\text{NRAr})_2$ (**4b**) is inert to several equivalents of tetrahydrothiophene or norbornylene at elevated temperatures ($80 \text{ }^\circ\text{C}$ in toluene). This lack of oxidizing ability is also reflected in the cyclic voltammogram of **4b**, which shows a quasi-reversible reduction 1.14 V negative of the $\text{Cp}_2\text{Fe}^{+/0}$ couple in CH_3CN . Scanning oxidatively, **4b** gives a value of $+0.409 \text{ V}$ for the $\text{OCr}(\text{OSiPh}_3)(\text{NRAr})_2^{+/0}$ redox couple. However, attempts to isolate the product of the reaction between **4b** and 1 equiv of various silver(I) salts did not give an isolable $[\text{OCr}(\text{OSiPh}_3)(\text{NRAr})_2]^+$ -containing product.

The dioxo $[\text{CoCp}_2][\text{O}_2\text{Cr}(\text{NRAr})_2]$ (**1**) reacts with benzoyl chloride to give moderate yields of the η^1 -benzoate complex $\text{OCr}[\text{OC}(\text{O})\text{Ph}](\text{NRAr})_2$ (**4c**). The hapticity of the benzoate ligand was confirmed by an X-ray crystal structure investigation

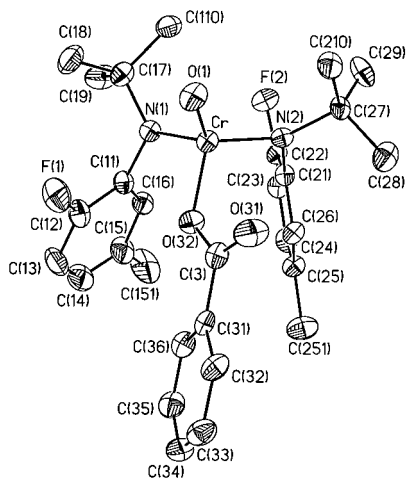


Figure 4. ORTEP diagram from the X-ray crystal structure data of $\text{OCr}[\text{OC}(\text{O})\text{Ph}](\text{NRAr})_2$ (**4c**). The ellipsoids are at the 25% probability level. Selected bond distances (Å): Cr–O1 1.588(3), Cr–N1 1.837(3), Cr–N2 1.832(4), Cr–O32 1.862(3). Selected bond angles (deg): O1–Cr–N2 116.9(2), O1–Cr–N1 108.7(2), N2–Cr–N1 112.7(2), O1–Cr–O32 110.3(2), N2–Cr–O32 108.1(2), N1–Cr–O32 98.5(2), C3–O32–Cr 125.7(3), C11–N1–C17 117.7(4), C11–N1–Cr 116.6(3), C17–N1–Cr 124.1(3), C21–N2–C27 116.7(3), C21–N2–Cr 111.2(3), C27–N2–Cr 131.5(3), O31–C3–O32 122.6(4).

(Figure 4). The structure indicates a Cr–O_{oxo} bond length of 1.588(3) Å, which is very similar to the Cr–O_{oxo} value in the chromium(VI) complex $\text{O}_2\text{Cr}(\text{NRAr})_2$ (**2**) and somewhat shorter than that found in $\text{OCr}(\text{OSiPh}_3)(\text{NRAr})_2$ (**4b**).

The monodentate benzoate is attributed to a combination of steric and electronic effects. The small chromium(V) metal center with two bulky anilides, an oxo ligand, and a monodentate carboxylate may be approaching coordinative saturation. In addition, if **4c** possesses a Cr–O_{oxo} triple bond, three σ -bonds to the ligands in the basal plane, two strong Cr–N_{amido} π -bonds, and an unpaired electron, it is a 17e complex. Bidentate coordination of the carboxylate ligand would give a “19e” complex. In short, an η^2 -benzoate residing in the basal plane would require the unfavorable weakening of the strong Cr–N_{amido} π -bonds.

3. Concluding Remarks

The treatment of $\text{Cr}(\text{NRAr})_3$ (**2**) with oxygen was found to result in oxidative loss of a single amido substituent, producing $\text{O}_2\text{Cr}(\text{NRAr})_2$ (**3**). Electron-rich **3** has a quasi-reversible Cr^{VI/V} redox couple at -1.14 V versus $\text{Cp}_2\text{Fe}^{+/0}$, and chemical reduction of **3** with cobaltocene gives stable $[\text{CoCp}_2][\text{O}_2\text{Cr}(\text{NRAr})_2]$ (**1**). The cobaltocenium salt **1** is the first example of a 4-coordinate dioxo with a 3d¹ electronic configuration. The dioxo radical anion reacts with the strong electrophiles MeOTf, ClSiPh_3 , and $\text{ClC}(\text{O})\text{Ph}$ forming the monooxo complexes $\text{OCr}(\text{OMe})(\text{NRAr})_2$ (**4a**), $\text{OCr}(\text{OSiPh}_3)(\text{NRAr})_2$ (**4b**), and $\text{OCr}[\text{OC}(\text{O})\text{Ph}](\text{NRAr})_2$ (**4c**), respectively. Structurally, the chromium(VI) dioxo complex (**3**) displays the shortest metal–oxo distance (average 1.591 Å) of this study befitting its higher formal oxidation state. Of the monooxo chromium(V) derivatives, $\text{OCr}[\text{OC}(\text{O})\text{Ph}](\text{NRAr})_2$ (**4c**) has a slightly shorter metal–oxo distance (~ 0.03 Å) and a slightly diminished average in metal–amido distance (~ 0.01 Å), indicative of the electron-withdrawing ability of benzoate relative to siloxide. Mayer and co-workers attribute the electrophilic nature of their d¹ complex $[\text{HB}(\text{pz})_3]\text{ReO}_2\text{Cl}^+$ to the positive charge;⁴ the nucleophilic nature of the d¹ compound $[\text{CoCp}_2][\text{O}_2\text{Cr}(\text{NRAr})_2]$ (**1**) can be

attributed to the negative charge in conjunction with the highly electron-donating amido substituents.

The conversion of an oxo substituent to a carboxylate or alkoxide ligand is a rarely explored route in inorganic synthesis. The generalization of this technique to related systems could provide a valuable tool for the study of oxo complexes. In addition, the elucidation of the properties of these compounds, especially carboxylate derivatives such as $\text{OCr}[\text{OC}(\text{O})\text{Ph}](\text{NRAr})_2$ (**4c**), in metathesis reactions may stimulate new studies in oxo chemistry.

4. Experimental Section

4.1. General Considerations. All manipulations were carried out in a Vacuum Atmospheres drybox under a purified nitrogen atmosphere unless stated otherwise. Anhydrous ether was purchased from Mallinckrodt and freshly distilled from purple sodium benzophenone ketyl. Toluene was purchased from Mallinckrodt and purified by refluxing over molten sodium under nitrogen for at least 2 days. Pentane (EM Science) was distilled from purple sodium benzophenone ketyl. Distilled solvents were transferred under vacuum to glass vessels and stored in a Vacuum Atmospheres drybox prior to use. All other solvents, including deuterated solvents, were degassed and stored over activated 3 Å sieves for at least 24 h before use. Sieves (3 Å) were activated by heating at approximately 200 °C in vacuo overnight. Benzoyl chloride was purchased from Aldrich Chemical Co. and was degassed prior to use. The ligand $\text{Li}(\text{NRAr})(\text{OEt}_2)$ was synthesized according to the literature procedure.¹⁵ Other chemicals were purchased from commercial sources and used as received.

The deuterated derivatives of the complexes were used in initial investigations and replaced with the all-protio derivatives in subsequent experiments/characterization.

¹H, ²H, and ¹⁹F NMR spectra were recorded on Varian XL-300 or Varian Unity-300 spectrometers. ¹H chemical shifts are reported with reference to solvent resonances (residual $\text{C}_6\text{D}_5\text{H}$ in C_6H_6 as 7.15 ppm) and were recorded at room temperature. ¹⁹F NMR chemical shifts are reported with reference to external CFCl_3 as 0.00 ppm. ²H NMR chemical shifts are reported relative to an external C_6D_6 reference. Combustion analyses were performed by Oneida Research Services, Whitesboro, NY, or by Microlytics, South Deerfield, MA.

4.2. Synthesis of $\text{Cr}(\text{NRAr})_3$ (2**).** In a 1 L round bottom flask equipped with a stir bar was loaded 370 mL of ether. The solvent was frozen in a liquid nitrogen temperature cold well. Once frozen, the flask was removed from the cold well and allowed to thaw on a stir plate until the solvent was a stirring slurry. To the cold solvent were added solid CrCl_3 (4.30 g, 27.2 mmol, 1.1 equiv) and $\text{Li}(\text{NRAr})(\text{Et}_2\text{O})$ (19.82 g, 73.9 mmol, 3.0 equiv). The solution was stirred and allowed to warm. Before reaching room temperature, the solution darkened to the dark brown of the product. The reaction was stirred overnight.

The next morning, the volatiles were removed in vacuo, giving a black powder. The powder was extracted into pentane, and the solution was filtered through a sintered glass frit using Celite as a filtering agent. The filter cake was washed with additional pentane until the filtrate was almost colorless, leaving gray LiCl and excess purple CrCl_3 in the frit. The dark filtrate was concentrated and cooled to -35 °C, which afforded the product as a black powder. The yield was 14.07 g (23.03 mmol, 93.5%), collected in four crops. Data collected on the deuterated derivative: ²H NMR (46 MHz, C_6D_6): δ 44.24 ppm ($\Delta\nu_{1/2} = 58$ Hz). Mp: 197–200 °C. EI MS (low resolution): m/z (%) 610 (38.26) [M^+]. μ_{eff} (300 MHz, C_6D_6 , 22 °C): 4.05 μ_{B} . Anal. Calcd for $\text{CrN}_3\text{F}_3\text{C}_{33}\text{H}_{27}\text{D}_{18}$: C, 64.89; H, 7.43; N, 6.88. Found: C, 65.38; H, 7.27; N, 6.80.

4.3. Synthesis of $\text{O}_2\text{Cr}(\text{NRAr})_2$ (3**).** Into a 250 mL glass bomb equipped with a stopcock and glass joint was loaded **2**, a stir bar, and 50 mL of ether. The glass joint was equipped with a septum and removed from the box. To the headspace was added 217 mL of O_2 at STP via syringe with stirring. The brown solution quickly changed to dark purple. The solution was stirred for an additional 30 min. The

Table 1: Crystallographic Data for O₂Cr(NRAr)₂ (**3**), OCr(OSiPh₃)(NRAr)₂ (**4b**), and OCr[OC(O)Ph](NRAr)₂ (**4c**)

| | 3 | 4b | 4c |
|---|--|---|--|
| empirical formula | C ₂₂ H ₃₀ CrF ₂ N ₂ O ₂ | C ₄₀ H ₄₅ CrF ₂ N ₂ O ₂ Si | C ₂₉ H ₃₅ CrF ₂ N ₂ O ₂ |
| <i>a</i> (Å) | 10.173(4) | 9.6227(9) | 19.061(6) |
| <i>b</i> (Å) | 13.758(6) | 10.3217(10) | 16.390(4) |
| <i>c</i> (Å) | 16.102(3) | 19.649(2) | 9.177(3) |
| α (deg) | 90 | 80.855(2) | 90 |
| β (deg) | 92.86(2) | 81.889(2) | 90 |
| γ (deg) | 90 | 72.625(2) | 90 |
| <i>V</i> (Å ³) | 2250.8(14) | 1828.2(3) | 2867(2) |
| <i>Z</i> | 4 | 2 | 4 |
| fw | 444.486 | 703.8939 | 533.60635 |
| space group | <i>P</i> 2 ₁ / <i>n</i> | <i>P</i> 1 | <i>Pna</i> 2 ₁ |
| ρ _{obsd} (g cm ⁻³) | 1.312 | 1.297 | 1.273 |
| μ (mm ⁻¹) | 0.544 | none measured | 0.443 |
| <i>F</i> (000) | 936 | 742 | 1156 |
| GOF ^a on <i>F</i> ² | 1.212 | 1.171 | 1.126 |
| R1(<i>F</i> _o) ^b for <i>I</i> > 2σ(<i>I</i>) | 0.0451 | 0.0887 | 0.0507 |
| wR2(<i>F</i> _o) ^c for <i>I</i> > 2σ(<i>I</i>) | 0.0948 | 0.1745 | 0.1284 |

$$^a \text{GOF} = [\sum[w(F_o^2 - F_c^2)^2]/(n - p)]^{1/2}. \quad ^b R1 = \sum||F_o| - |F_c||/\sum|F_o|. \quad ^c wR2 = [\sum[w(F_o^2 - F_c^2)^2]/\sum w(F_o^2)^2]^{1/2}.$$

volatiles were removed in vacuo. Recrystallization from pentane at -35 °C yielded black crystals (1.083 g, 2.44 mmol, 83% yield). X-ray quality crystals were obtained from a concentrated ether solution cooled to -35 °C. ¹H NMR (300 MHz, CDCl₃, 25 °C): δ = 1.18 (s, 9H, C(CH₃)₃), 1.29 (s, 9H, C(CH₃)₃), 2.18 (s, 6H, ArCH₃), 2.30 (s, 6H, ArCH₃), 6.49 (d, 1H, *o*-Ar), 6.96 (m, 5H, Ar). ¹⁹F NMR (300 MHz, CDCl₃, 25 °C): δ = -118.28, -118.85. EI MS (low resolution): *m/z* (%) 444 (1.6) [*M*⁺]. Anal. Calcd for C₂₂H₃₀CrF₂N₂: C, 59.45; H, 6.80; N, 6.30. Found: C, 59.98; H, 7.01; N, 5.93. The derivative with deuterated butyl groups was produced analogously.

4.4. Synthesis of [CoCp₂][O₂Cr(NRAr)₂] (1**).** O₂Cr(NRAr)₂ (**3**) was made without purification from Cr(NRAr)₃ (**2**) (0.503 g, 0.847 mmol) and O₂ (2.6 mL at STP, 3 equiv) in a 250 mL bomb as described above. After stirring, the volatiles were removed in vacuo to give a purple solid. The bomb was returned to the drybox, and 15 mL of C₆H₆ was added to dissolve the crude **3**. To the stirring solution was added CoCp₂ (0.160 g, 1 equiv) in ~3 mL of C₆H₆, dropwise. As the reductant was added, the product precipitated. After addition was complete, the bomb was sealed and shaken by hand for 5 min. The product was collected by filtration on a fritted glass filter and washed with 3 × 20 mL of ether. The solid was dried under vacuum to yield 0.476 g (89%) of light brown powder. The compound is pure enough to be used in further synthesis after washing but may be recrystallized from carefully dried THF, if necessary. Data on the derivative without deuterium label: Anal. Calcd for C₃₂H₄₀CoCrF₂O₂N₃: C, 60.66; H, 6.36; N, 4.42. Found: C, 60.97; H, 6.46; N, 4.23. The derivative with deuterated butyl groups was produced analogously. ²H NMR (300 MHz, THF): δ = 2.12 ppm (Δ*ν*_{1/2} = 30 Hz).

4.5. Synthesis of OCr(OMe)(NRAr)₂ (4a**).** In a 20 mL vial, deuterated dioxo complex **1** (0.425 g, 0.657 mmol, 1 equiv) was slurried with 10 mL of toluene. The slurry was frozen in a liquid nitrogen temperature cold well in the drybox and then allowed to warm until it could be stirred. With stirring, MeOTf (75 μL, 0.663 mmol, 1 equiv) in ~2 mL of toluene was added dropwise. As the reaction warmed, the solution changed color from the light brown of the dioxo complex to deep blue. The reaction mixture was stirred for ~10 min at room temperature before removal of the volatile material in vacuo. The blue-green complex was extracted into pentane and filtered to remove yellow [CoCp₂][OTf]. The complex was purified by recrystallization from pentane to give black blocks in 76% (0.235 g) yield. Data on the derivative without deuterium label: Anal. Calcd for C₃₂H₄₀CoCrF₂O₂N₃: C, 58.58; H, 7.05; N, 5.94. Found: C, 59.05; H, 7.31; N, 5.84. Data on the deuterated derivative: EI MS (low resolution), *m/z* (%) 471 (0.2) [*M*⁺]. ²H NMR (300 MHz, pentane): δ = 3.20 ppm (Δ*ν*_{1/2} = 78 Hz), ~3.8 ppm, 6.06 ppm (Δ*ν*_{1/2} = 190 Hz).

4.6. Synthesis of OCr(OSiPh₃)(NRAr)₂ (4b**).** In a 20 mL vial, dioxo complex **1** (0.168 g, 0.265 mmol, 1 equiv) was slurried with 10 mL of toluene. The slurry was frozen in the cold well and then allowed to warm until it could be stirred. With stirring, ClSiPh₃ (78 mg, 0.265 mmol, 1 equiv) in ~2 mL of toluene was added dropwise. As the

reaction warmed, the solution changed color from the light brown of the dioxo complex to deep blue. The reaction mixture was stirred for ~10 min at room temperature, and then the volatiles were removed in vacuo. The blue-green complex was extracted into pentane and filtered to remove yellow [CoCp₂][Cl]. The complex was purified by recrystallization from pentane to give black plates in 86% (0.161 g) yield. X-ray quality crystals were obtained from a concentrated pentane solution cooled to -35 °C. Data on the derivative without the deuterium label: EI MS (low resolution): *m/z* (%) 703 (0.2) [*M*⁺]. Anal. Calcd for C₄₀H₄₅CrF₂O₂N₂Si: C, 68.26; H, 6.44; N, 3.98. Found: C, 68.67; H, 6.55; N, 3.82. Data on the deuterated derivative: ²H NMR (300 MHz, toluene, 25 °C), δ = 0.21 ppm (Δ*ν*_{1/2} = 28 Hz, ~1H), 2.07 ppm (Δ*ν*_{1/2} = 40 Hz, ~1H), 4.51 ppm (Δ*ν*_{1/2} = 65 Hz, ~1H).

4.7. Synthesis of OCr[OC(O)Ph](NRAr)₂ (4c**).** A slurry of **1** (1.000 g, 1.549 mmol, 1 equiv) with 40 mL of THF was prepared and frozen in a liquid nitrogen temperature cold well. The frozen solution was allowed to warm until it could be stirred with a magnetic stir bar. A cold solution of benzoyl chloride (180 μL, 1.551 mmol, 1 equiv) in 10 mL of THF was added dropwise over a few minutes. A rapid color change occurred during the addition to produce a dark blue solution. After 1 h of stirring, the volatiles were removed in vacuo. The resulting black solid was extracted with pentane and then filtered through a fritted filter. The filtered solution was cooled to -35 °C overnight. A black powder precipitated, which was collected on a frit and washed with -35 °C pentane. The black product was isolated in 34% yield (0.296 g) and makes dark green solutions when dissolved. X-ray quality crystals were obtained from a concentrated pentane solution cooled to -35 °C. Data on the deuterated derivative: EI MS (low resolution) *m/z* (%) 561 (0.96) [*M*⁺]. Anal. Calcd for C₂₉H₂₃CrF₂O₃N₂D₁₂: C, 61.67; H, 6.38; N, 4.81. Found: C, 62.01; H, 6.28; N, 4.99. ²H NMR (300 MHz, ether, 25 °C): δ = 6.43 ppm (Δ*ν*_{1/2} = 140 Hz, ~2H), 3.26 ppm (Δ*ν*_{1/2} = 50 Hz, ~1H), 0.78 ppm (Δ*ν*_{1/2} = 32 Hz, ~2H).

4.8. X-ray Crystal Data. Crystals grown from concentrated solutions at -35 °C quickly were moved from a scintillation vial to a microscope slide containing Paratone N (an Exxon product). Samples were selected and mounted on a glass fiber in wax and Paratone. The data collections were carried out at a sample temperature of 188 K on a Siemens Platform three-circle goniometer with a CCD detector using Mo Kα radiation (λ = 0.710 73 Å). The data were processed and reduced utilizing the program SAINT supplied by Siemens Industrial Automation, Inc. The structures were solved by direct methods (SHELXTL v5.03, Sheldrick, G. M., and Siemens Industrial Automation, Inc., 1995) in conjunction with standard difference Fourier techniques. All non-hydrogen atoms were refined anisotropically. Hydrogen atoms were placed in calculated (*d*_{C-H} = 0.96 Å) positions. Some details regarding reduced data and cell parameters are available in Table 1. In addition, selected bond distances and angles are supplied in the figure captions of ORTEP drawings.

4.9. General Considerations for SQUID Measurements. The solid-state magnetic measurements were performed with a Quantum Design

SQuID magnetometer using MPMSR2 software. The experiment was carried out at a field strength of 1000 G. The samples were loaded into no. 4 gelatin capsules and suspended in plastic straws. The sample was secured in the gel cap with a square of Parafilm. The measurements were done from 5 to 300 K with data points taken every 5 K. The sample was centered and measured using standard techniques. The data are corrected for sample diamagnetism using Pascal's constants and background from similar runs without sample. The data were fit using the equation $\chi_M = (\mu^2/(7.997584(T - \theta))) + \chi_{\text{tip}}$ (Curie–Weiss Law). The fit was carried out on a plot of χ_M vs T with μ , θ , and χ_{tip} as variables.

4.10. SQuID Data for [CoCp₂][O₂Cr(NRAr)₂] (1). $\mu_{\text{eff}} = 1.81(2)$ μ_B ; $\theta = -0.23(1)$ K; $\chi_{\text{tip}} = 2.1(1) \times 10^{-4}$; R (least-squares fit of χ vs T plot) = 0.99998.

4.11. SQuID Data for OCr(OMe)(NRAr)₂ (4a). $\mu_{\text{eff}} = 1.709(03)$ μ_B ; $\theta = -0.159(2)$; $\chi_{\text{tip}} = 3.36(2) \times 10^{-4}$; R (least-squares fit of χ vs T plot) = 1.00.

4.12. General Experimental Details for Cyclic Voltammetry. The electrochemical measurements were performed in ~ 1 M tetra-*n*-butylammonium hexafluorophosphate (TBAH) in THF or ~ 0.1 M TBAH in acetonitrile solution containing the compound of interest. In a typical experiment, 6–12 mg of the complex was dissolved in 0.75 mL of dry solvent. Then, this solution was added to the saturated TBAH solution. A platinum disk (1.6 mm diameter, Bioanalytical systems), a platinum wire, and a silver wire were employed as the working, the auxiliary, and the reference electrode, respectively. All measurements were performed in a one-compartment cell. The electrochemical response was collected with the assistance of an Eco-Chemie Autolab potentiostat (pgstat20) and the GPES 4.3 software. An IR correction drop was employed due to the high resistance of the solution (a typical resistance value measured with the positive feedback technique for these solutions was 975 Ω). All of the potentials are reported against the ferrocenium/ferrocene couple measured in the same solution.

4.13. Cyclic Voltammetry on O₂Cr(NRAr)₂ (3). A THF solution (0.75 mL) containing approximately 1 M TBAH and 8 mg of O₂Cr(NRAr)₂ (3) was prepared. Scanning reductively at a rate of 200 mV/s, a reversible wave was observed at a potential of -1.024 V, and a second irreversible wave was observed at a high reduction potential of

-2.9 V. The latter one is just below the reduction potential of the solvent. Once the second reduction wave had occurred (irreversible), new waves were observed when scanning oxidatively. Unfortunately, no reliable spectra could be obtained when scanning the same compound in 0.1 M TBAH in CH₃CN. A reversible reduction wave was found to appear and decay to other waves in the course of the experiments in acetonitrile. Complex 3 appears to rapidly decompose in this solvent.

4.14. Cyclic Voltammetry on OCr(OSiPh₃)(NRAr)₂ (4b). A THF solution (0.75 mL) containing approximately 1 M TBAH and 12 mg of OCr(OSiPh₃)(NRAr)₂ was prepared. Only scanning at high rates ($\sim 50\,000$ mV/s) resulted in an observable reduction wave. The potential for this wave was approximated to be -1.83 V. Also, an oxidation at approximately $+0.49$ V was observed at high scan rates. The oxidation wave was just below the solvent limit, which effected the reversibility of the spectrum. The wave appears to be quasi-reversible at high scan rates, but at lower scan rates no reversibility of this wave is observed. Acetonitrile solutions containing 0.1 M TBAH proved more amenable to study. When scanning reductively, a quasi-reversible wave can be observed at -1.19 V (vs FeCp₂^{0/+}, 100 mV/s). From scans at higher rates (200 mV/s) and oxidative/reductive current ratios it can be concluded that the wave was partially reversible. The oxidation couple OCr(OSiPh₃)(NRAr)₂^{0/+} was approximated as $+0.409$ V.

Acknowledgment. For funding C.C.C. thanks the National Science Foundation (CAREER Award CHE-9501992), DuPont (Young Professor Award), the Packard Foundation (Packard Foundation Fellowship), Union Carbide (Innovation Recognition Award), and 3M (Innovation Fund Award). C.C.C. is a Sloan Foundation Fellow (1997–2000). A.L.O. is grateful to Texaco for a fellowship.

Supporting Information Available: Cyclic voltammograms for 3 and 4b. X-ray crystallographic files in CIF format for 3, 4b, and 4c. This material is available free of charge via the Internet at <http://pubs.acs.org>.

IC981403R